

Morphodynamics of nearshore rhythmic sandbars in a mixed-energy environment (SW France): 2. Physical forcing analysis

V. Lafon^a, H. Dupuis^{a,*}, R. Butel^a, B. Castelle^a, D. Michel^a, H. Howa^b,
D. De Melo Apoluceno^a

^a *Département de Géologie et Océanographie, UMR EPOC 5805 (CNRS), Université Bordeaux I, Avenue des facultés, 33405 Talence Cedex, France*

^b *Université d'Angers, UFR Sciences, 2 Boulevard Lavoisier, 49045 Angers Cedex 01, France*

Received 17 February 2003; accepted 14 June 2005

Available online 24 August 2005

Abstract

The morphology and migration of rhythmic intertidal ridge and runnel systems, and subtidal crescentic bars that border the southwest coast of France were characterized using in situ surveys and maps obtained by remote-sensing methods. The period from 1986 to 2000 was investigated. A total of 35 km of coast was mapped. This data set shows several specificities, the origin of which are examined in the present report using hydrodynamic data. A complete analysis of the influence of wave climate on both the shape and the movements of these rhythmic sedimentary patterns was performed. In addition, SWAN and MORPHODYN-coupled numerical models were used to provide quantification of both wave breaking and longshore currents for wave parameters that were representative of the mean values and of the energetic conditions. This study demonstrated the short time response of intertidal systems to the wave forcing. When the offshore significant wave height (H_s) was lower than 2.5 m, regular coastal ridge and runnel systems developed in the intertidal zone and migrated in the longshore-drift direction at a rate of 1.7–3.1 m day⁻¹. By contrast, the ridge and runnel system morphology abruptly changed when the H_s exceeded 2.5 m, and after the storm, the typical ridge and runnel rhythmic topography was recovered within 5–9 days. The crescentic bars, which had a convex seaward shape, were affected by waves with H_s values greater than 3 m (slightly less for short waves). Depending on the wave orientation, the crescentic bars moved in the longshore-drift direction at a rate that reached 1 m day⁻¹. The data suggested a slight negative correlation between the mean alongshore length of the crescentic bar and the mean H_s . Finally, it seemed that increasing the wave obliquity with respect to the coast resulted in the flattening of the crescentic bars. Thus, coupling Spot and in situ mapping to hydrodynamic records allow the characterization of coastal morphology and dynamics, with time and space samplings that are particularly well adapted to the little studied alongshore morphodynamics. This approach should improve the difficult parameterization of morphodynamic models in high-energy environments.

© 2005 Published by Elsevier Ltd.

Keywords: Atlantic coast; rhythmic sandbank morphodynamics; ridge and runnel beach; sediment transport; Spot image analysis; subtidal crescents

1. Introduction

Increasing our morphodynamic knowledge of the coastal zone is essential for the development of beach-change models. These are required by decision makers to plan the development of the littoral zone, which is

* Corresponding author.

E-mail address: h.dupuis@epoc.u-bordeaux1.fr (H. Dupuis).

fragile but of high economic potential. This paper provides an innovative method for analyzing the alongshore morphology and dynamics of nearshore sandbars, which are common features along mesotidal and macrotidal sandy coasts that are exposed to oceanic waves. Nearshore bars frequently include regular or quasi-regular alongshore non-uniformities, which are collectively referred to as rhythmic topography. Beach cups (Coco et al., 2003), rip-current channels (Brander and Cowell, 2003) and crescentic bars (Van Enckevort and Ruessink, 2003b) are examples of nearshore rhythmic patterns that are repeated along the coast. A combination of several rhythmic systems in the cross-shore direction is commonly observed (Aagaard, 1991; Short and Aagaard, 1993). The morphology of nearshore sandbars evolves over time, and the changes in shape comprise alongshore uniform and non-uniform components. The former include onshore and offshore migrations (reviews by Shand et al., 1999 and Van Enckevort and Ruessink, 2003a). The latter encompass changes in quasi-rhythmic non-uniformities (Konicki and Holman, 2000; Van Enckevort and Ruessink, 2003b). These consist of alterations in length scale, cross-shore amplitude and alongshore migration. The results of the latest investigations, based on extensive video or field surveys coupled to wave-forcing analysis, have revealed the diversity in alongshore length (from a few meters to a few kilometers) and the behavior of these non-uniform features. They have also shown that the alongshore migration of nearshore bars is of the same order of magnitude ($1\text{--}10\text{ m day}^{-1}$) as the cross-shore migration of rhythmic patterns.

The SW sandy coast of France (about 200 km) exhibits two distinct rhythmic sedimentary systems that are repeated along the shore. Ridges that are regularly interrupted by runnels are found in the intertidal zone, whilst crescentic bars appear at about 500 m offshore the ridges and runnels in the subtidal zone. The morphology and dynamics of these bars have been extensively studied using both in situ surveys (Michel and Howa, 1999; De Melo Apoluceno et al., 2002; Desmazes et al., 2002) and remotely sensed maps (Froidefond et al., 1990; Lafon et al., 2002a, 2004). On a weekly scale, field investigations demonstrate that the shape of these rhythmic patterns changes over time, and that they are susceptible to movements both in the cross-shore and alongshore directions (the data and analytical results are summarized in Section 2). The yearly average alongshore lengths of the nearshore crescentic bars and ridge and runnel systems suggest that they are not under morphological control. However, satellite images and photographs often show two ridge and runnel systems coupled with one nearshore crescentic bar (Castelle and Bonneton, 2004). Although quantitative, these observations need to be explained and, particularly, to be precisely linked to the hydrodynamics, which is princi-

pally driven by the wave dynamics in this case. As wave estimates are obtained in deep water, numerical wave and hydrodynamic models describing the wave propagation towards the bars and the wave forcing at the bars were used here. An analysis of the meteorological and hydrological forcing is provided in Section 3. This paper aims to analyze the influence of wave climate on: (1) ridge and runnel shape; (2) ridge and runnel migration rate; (3) crescentic bar shape and (4) length scale; and (5) crescent-shaped bar alongshore migration rate. The results of this study are detailed in Sections 4–8. In the discussion (Section 9), the results are compared with the response of bars to wave forcing observed at other locations.

2. Study area

2.1. Physical settings

The Gironde coast forms the northern part of the SW coast of France (Fig. 1). It is about 120 km in length. In

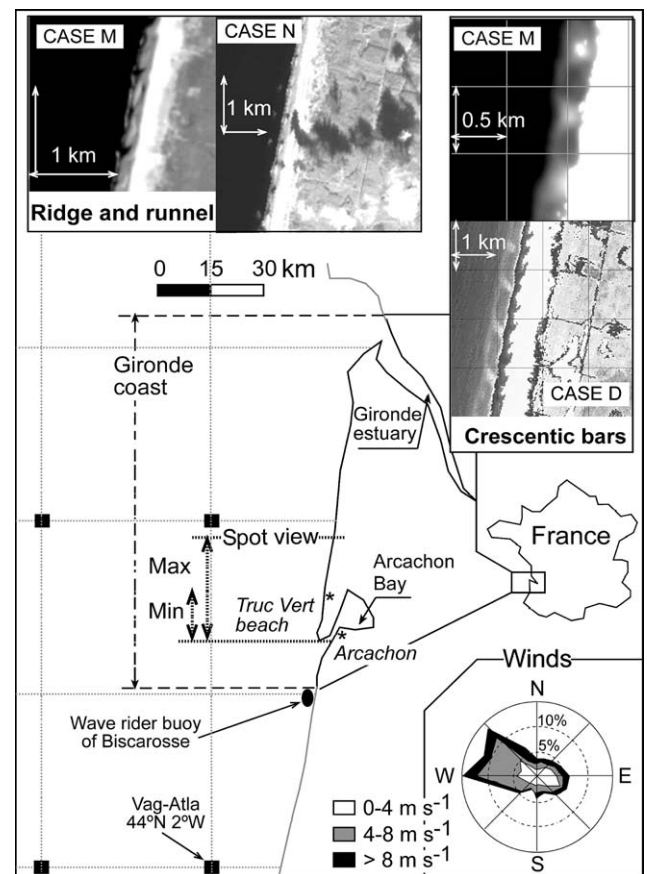


Fig. 1. Location of the study area, including Spot swath width. Four subs-scenes extracted around Truc Vert beach show the typical morphology of the ridge and runnels and of the crescentic bars. The Vag-Atla grid and the wave-rider buoy location are supplied together with a wind rose.

this area, the beaches are composed of homogeneous quartz sands, with mean grain sizes ranging from 200 to 400 μm (Pedreros et al., 1996). Rocks are uncommon, except in the vicinity of the inlet of the Gironde estuary. The semidiurnal tide generates clockwise rotating currents with speeds on the continental shelf that do not exceed 0.25 m s^{-1} (Lorin et al., 1979). Mean tidal and mean spring tidal ranges of 3.2 and 4.3 m, respectively, characterize the mesotidal to macrotidal environments (Davies, 1972).

Analysis of the records of the non-directional wave-rider buoy of Biscarosse (Météo-France), which is located about 10 km south of the study area (at a 26 m depth), shows that from October to March, the waves have a mean significant height (H_s) of 1.66 m and a mean significant period (T_s) of 9.6 s, whilst from April to September the mean H_s and T_s are 1.13 m and 7.45 s, respectively (Butel et al., 2002). Westerly to northwesterly waves, which are associated with long swells traveling from the North Atlantic Ocean, reach the coast more than 50% of the time. The mean wave height and mean tidal range indicate a mixed-energy environment of relatively high energy following the classification proposed by Davis and Hayes (1984).

To complement this overview of the forcing, an analysis of wind records for the period from 1987 to 1995 has been performed. The wind speed and direction recorded eight times per day by the French meteorological office (Météo-France) at Arcachon (to the south of the study site; cf. Fig. 1) were used for this purpose. The results show that northwesterly ($292.5\text{--}337.5^\circ$) to westerly ($247.5\text{--}292.5^\circ$) winds are dominant 46% of the time; 43% of the westerly winds are stronger than 5 m s^{-1} and 7% are stronger than 9 m s^{-1} . Annual easterly winds ($67.5\text{--}112.5^\circ$) account for 37% of the directions and the percentage of annual southwesterly winds ($157.5\text{--}202.5^\circ$) is 17%.

2.2. State-of-knowledge review of the morphology and dynamics of nearshore sandbars along the SW coast of France

2.2.1. Ridge and runnel

Three consecutive ridge and runnel systems have been monitored at Truc Vert beach (cf. Fig. 1) at 2-week intervals over a 4-year period (De Melo Apoluceno et al., 2002). The rhythmic topography is described as an alongshore succession of sand bars, with the northern part connected to the beach, which are regularly interrupted by channels that are SW-NE or SSW-NNE oriented. From May to September 1999, the ridges and runnels migrated eastward and southward at mean rates of 0.8 and 1.7 m day^{-1} , respectively. During this period, the average H_s and T_s of the waves were 1.2 m and 6.5 s, respectively. Short periods of waves with a wave height of 2–3 m have been observed sporadically, with the

maximum-recorded H_s being 3.2 m. According to these measurements, the southward transport rate in the ridge and runnel area (Q_l) ranged from 0.5 to $1.1 \text{ m}^3 \text{ m}^{-1} \text{ day}^{-1}$ (Lafon et al., 2004).

To complement these surveys in space and time, 16 high-resolution Spot scenes (Table 1) have been explored (Lafon et al., 2002a, 2004). In Table 1, a letter is assigned to each scene. In the text, the letters are used to refer to the scenes and to the derived maps. These allowed the mapping of up to 37 km of shoreline directly north of the Arcachon inlet (cf. Fig. 1). The ridge and runnel system shape was delineated at the lower astronomical tide (LAT) using a bathymetric model that provides the shallow-water depth with an accuracy of 20% (Lafon et al., 2002b). In general, spatial maps show contiguous patterns of intertidal systems (Fig. 1, case M), the mean distance between successive runnel axes ranges from $370 \pm 15 \text{ m}$ (the variability is indicated by the standard error in the text) to $463 \pm 25 \text{ m}$ according to the image. In cases N (cf. Fig. 1) and O, the Spot contours exhibit bars that are interrupted by arbitrarily orientated runnels, which are also observed in the field. The two Spot scenes recorded in the summer of 1989 (07/29 and 10/04) were used to derive the alongshore ridge and runnel migration rate (Lafon et al., 2002a). The extracted coastlines showed comparable shapes that shifted in the alongshore direction. During this period, the mean wave height and period were 1.05 m and 7.9 s, respectively. Waves that were higher than 2 m were observed less than 5% of the time and the wave height reached a maximum of 3.3 m. In July and October, 80 and 81 systems were identified, respectively, 83% of which exhibited quasi-unchanged shapes; among these, 84% moved south at a mean speed of $2.4 \pm 2.1 \text{ m day}^{-1}$ with an accuracy of 12%. The southward transport rate (Q_l) ranged from 0.74 to $1.5 \text{ m}^3 \text{ m}^{-1} \text{ day}^{-1}$ (Lafon et al., 2004).

2.2.2. Crescentic bars

Subtidal sandbanks were mainly studied by remote-sensing methods. Nine crescentic plan shapes were examined (Lafon et al., 2004). Crescentic bedforms, which were linked by wing-type elevated end sections (horns), commonly exhibited a convex seaward shape (Fig. 1, case M). In one case, flattened bars, comprising a linear north section that was NNE-SSW oriented and a linear south section that was oriented nearly NW-SE, were observed (Fig. 1, case D). In the area of investigation, and based on this data set, the length scale of the crescentic bars, which was defined as the distance between successive horns, ranged from 579 ± 28 to $818 \pm 33 \text{ m}$ (these data represent the average and standard error over the systems, with an accuracy of 60 m). Two pairs of crescentic plan shapes were used to study the alongshore migration of the subtidal bars. The crescentic plan shape from 20 April

Table 1

Orientation of runnels in comparison to the shore, shape of the subtidal crescentic bars, wavelength and alongshore migration rate of both the rhythmic sedimentary forms deduced from spatial maps. The number of systems used to derive bar topography and dynamics is also supplied

Date	Case	Ridge and runnel systems						Crescentic bars			
		Runnel angle	Length scale (m)	Accuracy (%)	Number of systems	Alongshore migration rate (m day ⁻¹)	Accuracy (%)	Shape	Length scale (m)	Number of systems	Alongshore migration rate (m day ⁻¹)
1986/07/16	A	20°	370 ± 15	6	91	3.1 ± 2.3	13	Convex	804 ± 32	40	1 ± 0.9
1986/09/02	B	20°	427 ± 14	3	85						
1989/07/29	C	20°	435 ± 23	5	81	2.4 ± 2.1	12	Flattened	777 ± 34	39	
1989/10/04	D	20°	430 ± 22	5	86						
1990/07/04	E	20°	390 ± 13	3	83						
1991/05/27	F	20°						Convex	818 ± 33	41	
1991/09/08	G	20°	426 ± 20	5	74			Convex	706 ± 26	44	
1992/05/18	H	20°	462 ± 28	6	45			Convex	726 ± 41	22	
1994/10/05	I	20°	419 ± 16	4	84						
1995/06/28	J	20°	421 ± 23	5	42						
1997/08/23	K	20°	440 ± 17	4	72						
1998/06/24	L	20°	404 ± 15	4	81			Convex	579 ± 28	51	
1999/07/16	M	20°	410 ± 19	5	79			Convex	633 ± 36	44	
1999/11/11	N	Random									
2000/04/20	O	Random						Convex	692 ± 40	39	0
2000/08/01	P	20°	463 ± 25	5	67			Convex	692 ± 37	45	

2000 precisely matched that from 1 August 2000, which suggests that the crescentic bars did not move during this period. By contrast, a southward shift of the bars was observed between 27 May and 8 September 1991 (Lafon et al., 2002a). In fact, 30 and 31 crescentic bars were observed in May and September, and about 91% presented similar plan shapes on both surveys. During this period, about 13% of the crescents maintained the same length, whilst in roughly 45 and 42% of the cases, their length increased by 133 m on average and decreased by 132 m on average. Finally, about 90% of the crescentic bars moved to the south at an average speed of 1 ± 0.9 m day⁻¹ (with an accuracy of 11%).

3. Meteorological and hydrological forcing analysis

3.1. Wave database

The H_s and T_s have been recorded since 1980 by the non-directional Datawell buoy of Biscarosse (Météo-France). This data set is discontinuous. To supplement the wave in situ measurements, wave climate (including wave direction) was used according to the Vag-Atla numerical model developed by Météo-France (AVISO database). Vag-Atla is a deep-water wave-prediction model that has produced wave forecasts four times per day over the Atlantic since 1996 (Guillaume, 1987). The output at the nearest grid point (44°N 2°W) was extracted (cf. Fig. 1). In this study, the wave-rider buoy data, when available, were used in preference; otherwise, the numerical model data were used after corrections for

statistical bias, allowing the best fit of the data in terms of H_s and T_s (Butel et al., 2002).

3.2. Nearshore waves and currents

3.2.1. Hydraulic models

As the wave characterization was only provided offshore, two nested models were used to estimate the order of magnitude of the hydrodynamic forcing on the two domains of interest: the subtidal and intertidal bars. Providing numerical simulations to correct each wave sample is beyond the scope of this paper, as these models need to be calibrated. Three results have been particularly emphasized: the changes in wave properties from the initial measurement location (buoy and simulated buoy) to the area located just before the crescentic bars; the location of wave breaking, which plays a major role in sediment re-suspension; and finally, the longshore currents allowing sediment transport.

The one-dimensional (1D) mode of SWAN40.11, which describes the wave-action density from the deep water to the surf zone, was used to quantify the evolution of the wave properties from the measurement location to the entrance of our domain. This model was set to take into account the bottom friction (Madsen et al., 1988) and the wave breaking according to Battjes and Janssen (1978). The other source terms were switched off for these runs. For the wave input, a frontal Gaussian-shaped frequency spectrum was used. In accordance with Butel et al. (2002), various values of the mean wave period (T_m ; 7.8 and 11 s) and the H_s (1, 2 and 3 m) were tested. Wave incidence, that perpendicular to the shoreline, was set to 10 or 30°. For these

simulations, the continental shelf was idealized from a depth of -110 to -5 m, including the slope variations defined by Desmazes et al. (2002). Initial depths of -55 and -110 m were chosen for mean wave periods of 7.8 and 11 s, respectively. This allowed the ratio of depth over wavelength at the input of the domain to be constant ($h/L_0 = 0.6$), thereby defining the beginning of the intermediate water. Also, meshes of the computational grid were varied with the wave period in order to obtain 115 grid points. Meshes of about 133 and 333 m were defined for wave periods of 7.8 and 11 s, respectively. A two-dimensional (2D) horizontal hydrodynamic model, based on the Saint Venant equation and called MORPHODYN (Saint-Cast, 2002), was coupled to the SWAN model in order to quantify the wave-induced longshore currents. Complete semidiurnal tidal cycles, with tidal ranges of 3 and 5 m, were simulated. The results of the runs are displayed in the following sections.

3.2.2. Run results

Fig. 2 shows the evolution of the ratio of wave heights H/H_0 (the subscript 0 stands for the input of the domain) as a function of the normalized water depth (h/L_0) at low tide, considering a tidal range of 5 m. The linear model, which does not include bottom friction (upper curve), reveals the effect of the de-shoaling that is responsible for a maximum loss in H_s of about 9% at an h/L_0 of 0.15, independently of the wave conditions. Two non-linear processes affect the other four curves. First, the continuous decrease in H_s is directly linked to the bottom friction. Clearly, the effect of bottom friction increases with decreasing wave periods. This can be explained by the fact that, over identical distances, short-period waves oscillate more often over the bottom than do long-period waves, which might amplify the effect of bottom friction. Second, at a given depth, a significant number of the waves start to break, leading

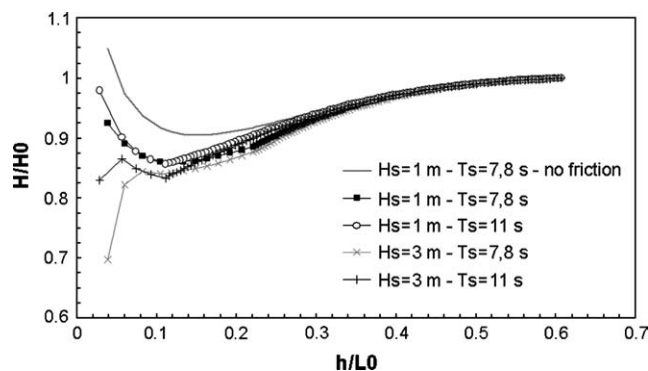


Fig. 2. Simulations of normalized water depth as a function of wave heights provided by SWAN for significant wave heights (H_s) of 1 and 3 m and significant wave periods (T_s) of 7.8 and 11 s. The upper curve displays the unique solution (independent of H_s and T_s) while bottom friction is neglected.

to a nearly linear decrease of H_s up to the coastline (Sénéchal et al., 2001).

Regarding the frequency of wave breaking in a 5-m depth, the results of the runs suggest that subtidal bars are not affected by wave breaking for 1 m H_s waves. For 2 m H_s waves, breaking is seen to be significant at the shortest T_m considered (7.8 s). For 3 m H_s waves, the wave-energy dissipation is significant regardless of the wave period. As a consequence, high waves with short periods that start breaking in a 5-m depth influence the evolution of the subtidal bars. By contrast, low-energy waves (H_s of 1 m) or moderate-energy waves with long periods (H_s of 2 m and T_m of 11 s) break in water depths shallower than 5 m and intense re-suspension will mainly affect the intertidal systems.

According to the MORPHODYN model, the sensitivity of longshore currents to the wave period is limited (less than 10%). On the contrary, the impact of wave direction and height is significant. For waves of 3 m height and 11 s period, the longshore current speed increases by a factor of three when the wave incidence increases from 10 to 30° . The maximum longshore current speeds are 0.62 and 0.92 m s^{-1} with H_s values of 2 and 3 m, respectively (with 11 s T_m and 30° incidence).

3.3. Wind database

To complete the discontinuous wave record provided by the buoy of Biscarosse before the Vag-Atla numerical outputs became accessible (the 1987 to 1995 period), wind speed and direction recorded at Arcachon (cf. Fig. 1) by Météo-France were investigated. This approach using the local wind forcing was found to be helpful for analyzing cases of duration-limited conditions, such as southerly or southwesterly winds. In such situations, the growth of waves is limited by the wind-event duration (D) and the wind speed. According to Carter (1982):

$$H_s = 0.0146 D^{5/7} U_{10}^{9/7} \quad (1)$$

$$T_p = 0.54 D^{3/7} U_{10}^{4/7} \quad (2)$$

where D is given in hours and U_{10} (greater than 5 m s^{-1}) is the wind speed at a height of 10 m. These relationships were first validated by comparing the H_s computation to the H_s value measured by the wave-rider buoy of Biscarosse. Wave periods were also compared to prove the generation of wind waves. Long-period swells were excluded. WSW to N storms, the beginning of which corresponded to relatively small waves, were selected. According to the D value, one (6–12 h), two (15–24 h) or three (24–54 h) computations were performed.

Twenty-five wind events were used to compute the H_s and the peak period (T_p). In all of the cases, the duration-limited condition was met. On 23 occasions,

the simulated T_p values were in the same range as the measured T_s values, particularly when considering the wave period at the end of the storms. In these cases, the root-mean-square (RMS) error obtained when establishing the regression between the measured and computed values of wave height decreased from 51 to 34 cm between the beginning and the end of the storms. The best RMS values were obtained when a minimum duration of 12 h and a minimum wind speed of 7 m s^{-1} were considered simultaneously. Therefore, the wave-height computation described by Carter (1982) tends to minimize the wave period and height, because it simulates only the pure-wind sea. It is particularly accurate for long-wind events with a minimum wind speed of 7 m s^{-1} . Taking these remarks into consideration, this method was used to calculate H_s for south directions and to discuss the eventual anomaly impact.

4. Ridge and runnel system shape modifications

4.1. Method

To explain the influence of the wave climate on ridge and runnel shape, the available wave parameters preceding each map were investigated. The period between the mapping and the first preceding storm was considered, going back in time a maximum of 2 months. Storm conditions ($H_s > 3 \text{ m}$) were defined on the basis of simulation results giving the percentage of wave breaking as a function of wave height (Section 3.2). The temporal variation of wave height, period and direction were examined to identify hydrodynamic and temporal thresholds that might determine abrupt modifications. Also, the time necessary for the systems to return to their regular shapes was assessed. Cases A, B and E have not been investigated because of the lack of wave measurements.

4.2. Results

Fig. 3 displays H_s , T_s and wave-direction data (when available) before each Spot map. According to the case (the occurrence of a storm), between 9 days and 2 months of data are shown. NNE to WSW waves were widely dominant. As the occurrence of SW waves was low (they were observed during less than 24 h for a few days preceding maps O and P), the short-term effect of wave incidence on the intertidal system is weakly indicated by our data set.

Initially, the dynamical thresholds associated with shape modifications were studied. Within the 10 days preceding maps N and O (on which randomly orientated runnels were noticed) storm events are clearly in evidence, with H_s and T_s values ranging from 2 to 4 m and from 7 to 9.5 s, respectively. In both cases, the mean

H_s was about 2.5 m. Considering the 10 days preceding the other maps, it appears that energetic events (either extremely short- or long-duration storms) always stopped at least 9 days before the mapping (cases K and M). During these 9 days, it was noted that: (1) the H_s never exceeded 2.5 m; (2) an H_s of 2 m was rarely reached and always for less than a few hours (C, L); (3) the T_s generally exceeded 8 s (except in cases L, M and P); and (4) the T_s usually reached 10 s and, less commonly, reached 12 s (C, F, G and J). This means that short and randomly oriented runnels appeared when the mean H_s exceeded 2.5 m (with wave periods of the order of 7 or 8 s). Also, it can be remarked that ridge and runnel systems were not perturbed for any T_s values (within the range from 7 to 12 s) if the wave height remained lower than about 1.5 m.

From this analysis, it can be deduced that if the ridge and runnel shape was affected by a storm, the bars and adjacent troughs recovered their classical summer shape in less than 9 days. About 9 and 4 days before map N (irregular shape), two distinct events characterized by high and long waves occurred. This means that the ridge and runnels were formed within 5–9 days after the storm.

5. Ridge and runnel system alongshore migration rate

Based on the Spot and in situ mapping, it was shown that the ridge and runnel migration rate varied significantly over time. A rate of about 1.2 m day^{-1} was obtained in 1999 (31 May–13 September), whilst it was about twice as high in 1989 (29 July–4 October). Fig. 4 displays the occurrences of H_s (a) and T_s (b) obtained from the wave gauge of Biscarosse for the 1989 investigation period (gray area) and those provided by Vag-Atla modified to reconstruct the Biscarosse buoy for the 1999 period (black area). The wave heights were slightly higher in 1999 than in 1989, whilst the wave periods recorded in 1989 exceeded those simulated in 1999 by about 19% (1.2 s on average). According to the MORPHODYN simulations, and considering such a low difference between the T_s values, the sand-transport migration rate must have been more influenced by the wave incidence than by the wave period. As the wave orientation for the 1989 period was not known, the data from 1999 (the orientation of the waves plotted as a function of their height) were compared to the orientation of waves on the same dates compiled for the years 1996 to 2000 in order to provide the mean conditions (Fig. 4c and d, respectively). The orientations in 1999 differed from the mean conditions. On average, NNW and SSW sector waves (with H_s values lower than 2 m) were slightly more in evidence, whilst NW to W waves were widely dominant. This suggests that, on average, the wave incidence in 1989 might have been

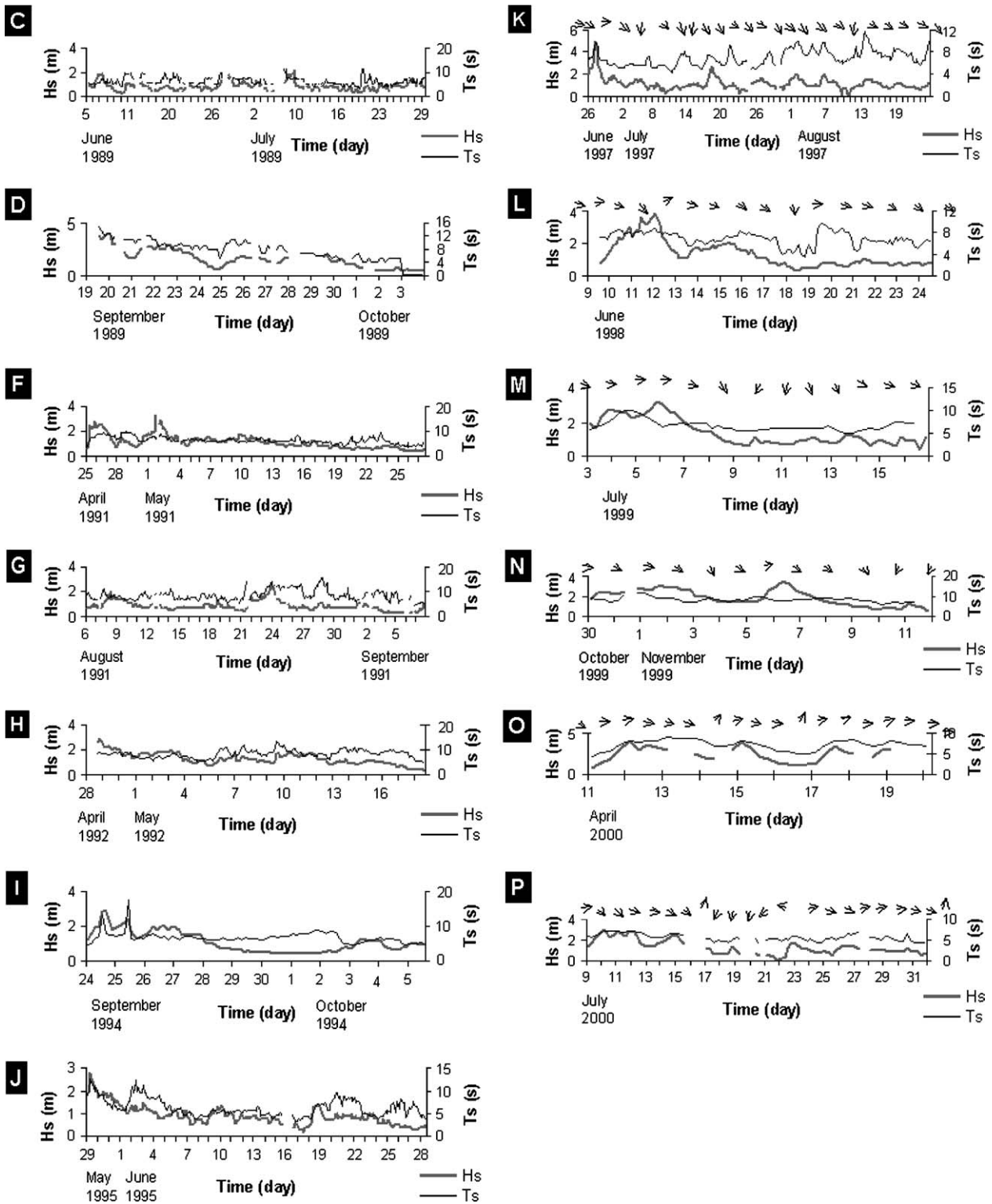


Fig. 3. H_s (large gray line), T_s (dark fine line) and wave propagation direction (arrows, when available), between each intertidal system mapping (presented chronologically) and the first preceding storm, going back in time up to maximally 2 months.

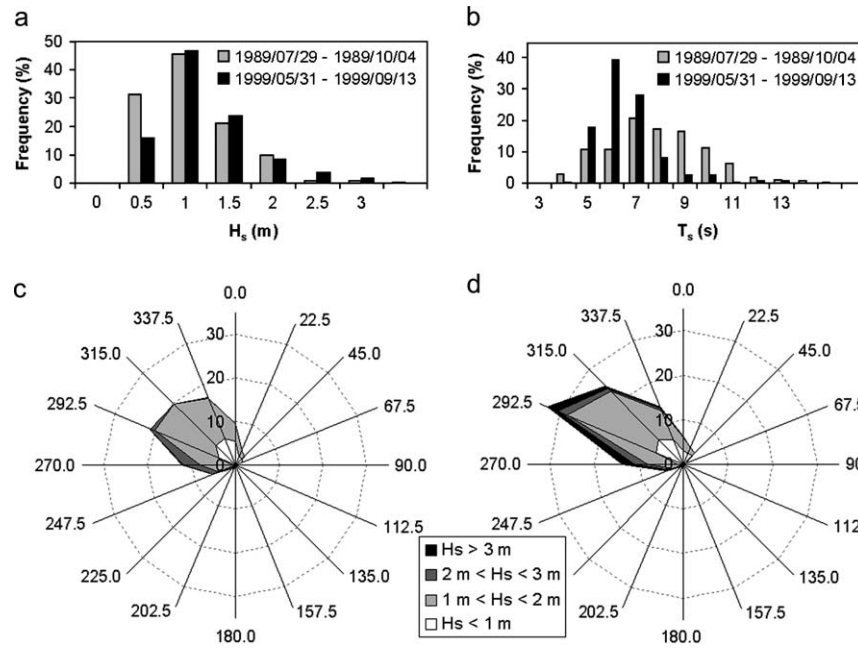


Fig. 4. Frequencies of significant wave height (a) and wave period (b) in summer 1989 (gray area) and summer 1999 (black area). Orientation of waves, plotted as a function of H_s , are displayed for the period 1999/05/31–1999/09/13 (c) and for the same date interval but compiling data from 1996 to 2000 (d).

more oblique than that in 1999 (characterized by an unusually small obliquity) allowing an increase in the alongshore migration rate.

6. Crescentic bar shape modifications

6.1. Method

Non-symmetrical bar shapes are logically linked to oblique waves that occur perpendicular to the coast (Blondeaux, 2001). To explain the occurrence of flattened crescentic bars along the SW coast of France in July 1989 (map C), wave statistics computed over the 12 months preceding map C were compared with 12-month wave statistics prior to cases F, G and H, which show convex bars. For this purpose, the H_s and T_s values obtained from the wave-rider buoy were investigated. Wave direction was not known. However, anemometer records compiled from 1987 to 1992 were used to estimate the formation of SW waves (the number of occurrences and height), which, due to the presence of the Spanish peninsula, are necessarily wind waves.

6.2. Results

Table 2 displays the SW wind events and induced wave heights (derived from Eq. (1)) for the period from 1987 to 1992. The in situ wave climate is shown for

comparison. In 1987, according to the wind database and the formula proposed by Carter (1982), significant SW waves were not in evidence. From January 1988 to May 1989, 19 episodes of SW winds able to generate SW waves were recorded. Among these, four occurred between January and July 1988, and the 15 remaining episodes occurred between September 1988 and May 1989. In all of the cases, following the validation approach described in Section 3.3, it was verified that the Biscarosse buoy recorded short-period waves. Also, the duration-limited condition was always met. Over the 6-month period preceding the maps, the comparison between the calculated and measured H_s and T_s values showed the following:

- Map C (May 1989), three major wind events were seen to induce WSW to W waves, the amplitude of which allowed them to break on the crescents during several hours in February 1989 and April 1989. In five additional cases, the calculated H_s values reached 1.9–2 m. These might also have had a direct impact on sand mobilization, as the associated wave periods were short.
- Map F (May 1991), six SW wind events were observed. Only one was associated with waves higher than 2 m.
- Map G (September 1991), SW winds were not detected.
- Map H (May 1992), five SW wind events associated with H_s values lower than 1.5 m were counted.

Table 2

SW wind events (190–280°) that occurred from January 1988 to May 1992. They are characterized by duration (D) and wind speed at a height of 10 m (U_{10}). They induce waves of significant wave height H_s , and of peak period T_p . Measured H_s and measured significant wave period (T_s) characterize observed waves. Double bars indicate Spot map dates

Episode number	Date	D (h)	U_{10} (m s ⁻¹)	Max comp. H_s (m)	Max comp. T_p (m)	Measured H_s range (m)	Measured T_s range (s)
1	1988/01/25	21	8	1.9	6.2		
2	1988/02/1–2	15	9	1.7	6	3.1–6.1	9–13
3	1988/04/12	18	7	1.4	5.7	1.8–2.6	5–7
4	1988/07/2–3	30	7	2	6.9	2–4.8	7–10
5	1988/09/1–2	21	8	1.9	6.5	2.9–3.6	8–10
6	1988/09/23–24	15	7	1.2	5.2	2.1–2.8	7–9
7	1988/10/5	18	9	1.9	6.5	1.4–3	7–11
8	1988/10/11–12	27	8	1.9	7.3	1.7–4.9	7–11
9	1989/01/6	9	6	0.7	3.9		
10	1989/01/21–22	12	6	0.9	4.4	1.8–2.2	6–8
11	1989/02/25–27	48	13	6.3	12.6		
12	1989/03/2	9	7	0.9	4.2		
13	1989/03/3	12	10	1.7	5.8		
14	1989/03/16	6	6	0.5	3.2	2.4–2.5	8–10
15	1989/04/1	6	7	0.6	3.5	1.4–1.6	7
16	1989/04/6	6	8	1.2	3.8		
17	1989/04/11–13	48	8	3.4	8.3	2.1–4.5	9–11
18	1989/04/16–17	24	12	3.5	12.1		
19	1989/05/12	30	3	1.7	6.5		
20	1990/09/21	18	5	0.9	4.7	1.4–2.2	6.3–8.8
21	1990/10/26–28	57	7	3.1	9.2	3.2–5.1	8–9.7
22	1990/11/01	6	7	0.7	3.5		
23	1990/11/20	9	7	0.9	4.2	2–2.3	7.1–8.2
24	1991/01/06	9	7	0.9	4.2		
25	1991/02/15	9	6	0.7	3.9	0.7–1.8	3.8–5.7
26	1991/09/28	9	8	1	4.5	3.2–5	9.8–15.5
27	1991/10/14	21	6	1.3	5.5	1.7–3.5	10.1–11.1
28	1992/01/09	12	8	1.2	5.1		
29	1992/03/12–13	18	5	0.9	4.7	1.9–2.8	9.4–13.8
30	1992/04/1–2	24	6	1.4	5.9	0.7–2.9	9.1–12.2

To summarize, recurrent and unusually strong southwesterly winds were recorded during the 8 months preceding the observation of linearly shaped crescentic bars, which are uncommon along the Atlantic SW coast of France. In many cases, these winds generated SW wind seas the height of which was sufficient to break over the crescentic bars and have an impact on their shape (cf. Section 3.2).

7. Length scale of the crescentic bars

The alongshore length of the crescentic bars changed over time (cf. Table 1). From 1986 to 1992, they were generally long with mean length scales varying from 706 to 818 m. Six years later, in 1998, their mean length scale was as small as 579 m. In fact, between 1992 and 1998, the number of crescentic bars longer than 800 m decreased by three-quarters. Finally, from 1998 to 2000, their spacing increased up to 692 m. Wave-climate modifications were investigated to explain the shortening and the lengthening of the crescentic bars. A

12-month period (including the winter months) was considered prior to each map. In some cases (SW high winds; cf. Section 3.3), the wind database was used to assess missing wave parameters. Based on these data, it appears that the mean length scale of the crescentic bars is negatively correlated with the mean H_s ($r = -0.76$; Table 3). Although the influence of T_s or wave incidence cannot be confirmed, they obviously play a role in the scatter as well as the initial state before a given hydrodynamic annual condition.

8. Crescentic bar alongshore migration rate

Crescentic bar alongshore movements did not occur systematically. Based on the Spot maps, deformations and motions were clearly in evidence from May to September 1991, whilst, on the contrary, crescentic bars were unchanged from April to August 2000 (cf. Table 1), at least at the scale of the observation (20×20 m pixels).

Table 3

Characterization of crescent mean length scale as a function of mean significant wave height (H_s), mean significant wave period (1986–1992) and mean wave period (1998–2000) T . σ_{H_s} and σ_T represent the standard deviation on H_s and T , respectively

Map date	Crescent mean length scale (m)	% $H_s > 3\text{m}$	Mean H_s (m)	σ_{H_s}	Mean T (s)	σ_T
1986/7/16	804	3.84615	1.42668	7.67357	0.827853	2.33524
1989/7/29	777	2.88960	1.43139	8.73580	0.844916	2.62432
1991/5/27	818	2.8868	1.28917	8.05155	0.751499	2.48452
1991/9/8	706	2.51148	1.30519	8.38444	0.770334	2.53706
1992/5/18	726	3.70461	1.31973	10.0772	0.805556	3.26764
1998/6/24	579	5.02630	1.70367	8.78443	1.03307	1.57284
1999/7/16	633	3.71901	1.78517	7.79948	0.880260	1.72342
2000/4/20	692	2.93160	1.64455	7.33430	0.924945	1.65121

Between May and September 1991, wave-gauge records from 7 June to 8 July were missing. The remainder of the data set was used and compared with wave conditions corresponding to the year 2000 data extracted from the Vag-Atla database (Fig. 5a, b). Waves with H_s values ranging from 2 to 3 m were observed more frequently in 2000 than in 1991. Furthermore, in 2000, more than 58% of the waves with H_s values ranging from 2 to 3 m presented T_s values shorter than 8 s, which seemed able to break on the crescentic bars (see Section 3.2). On the contrary, the H_s values were always lower than 3 m in 2000, while H_s values higher than 3 m occurred 2.3% of the time in 1991. The occurrence of these energetic conditions might have favored the migrations of the bars. Wave incidence angles, for four classes of H_s , show that, in 2000, waves

with 2–3 m H_s were mainly from the W-WNW sector (Fig. 5c). The orientation is important, as null along-shore transportation might be the result of an equal repartition of NW to SW waves. The wave obliquity for the 1991 period is not known. However, the orientation of the waves plotted as a function of their height from 20 April 2000 to 1 August 2000 was compared with the orientation of waves on the same dates compiled for the years 1996 to 2000 to provide the mean conditions (Fig. 5d). This test shows that the orientations in 2000 were, on average, less oblique than those under the mean conditions. On average, the NW sector waves (with H_s values higher than 2 m) were slightly more common (by about one-third) in 2000, whilst NNW and N waves occurred two- and five-times less frequently. Therefore, the mean conditions favored the southward

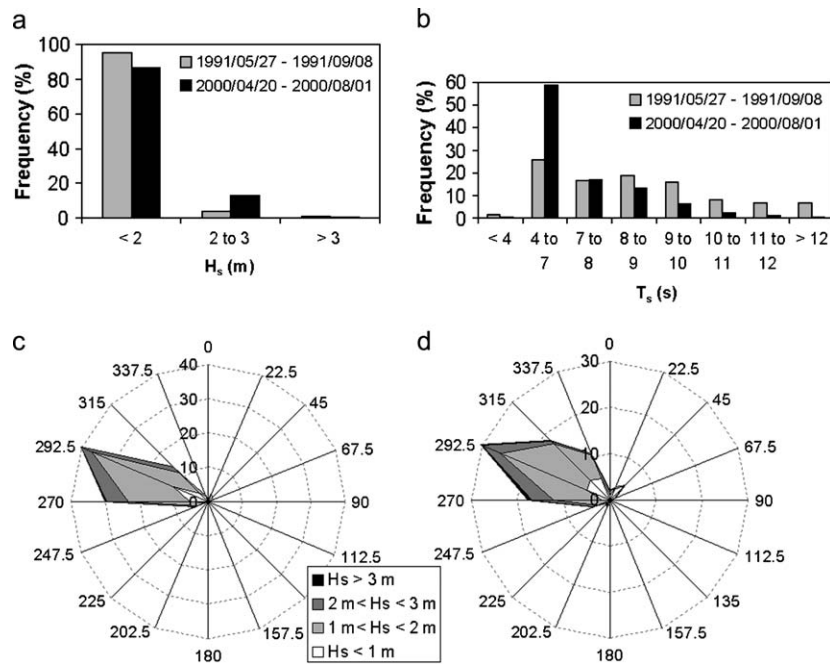


Fig. 5. Significant wave height (a) and wave period (b) frequencies from 1991/05/27 to 1991/09/08 (gray) and from 2000/04/20 to 2000/08/01 (black). Orientation of waves, plotted as a function of H_s , are displayed for the period 2000/04/20–2000/08/01 (c) and for the same date interval but compiling data from 1996 to 2000 (d).

migration of the bars. This suggests that, in 1991, the obliquity of the waves might have been comparable to the mean conditions.

9. Discussion

The investigation of various sources of hydrodynamic data was necessary in order to obtain a substantial and useful data set for explaining the morphology and dynamics of rhythmic sandbars that border the Gironde coast. Indeed, wave observations in the area were sparse and wave direction was not provided, except by numerical models and the recent data set. Comparing, for instance, the numerical simulation results (or the empirical results for wind-wave generation) with the in situ data required a careful analysis of eventual biases. For instance, in this study, a statistical correction was applied to estimate the wave-rider buoy records based on the Vag-Atla outputs, as the numerical results concerned only a few case studies with idealized bottom morphology. As another example, the formula proposed by Carter (1982) was used to simulate the wave heights produced by winds. It was validated in the case of the SW coast of France; however, this study proved that it must be used with care. This formula generally underestimates wave height, as the computations initially refer to a theoretical flat sea surface. However, it provides useful results for formulating hypotheses concerning coastal morphodynamics.

Sediment transport in the nearshore area results from complex interactions between cross-shore and along-shore processes. Across the shore, the onshore component results from the wave-asymmetry effect. The seawards-directed flux is caused by undertow, which balances the onshore mass transport associated with waves propagating towards the shore. In relation to this bi-directional flux, the nearshore bars move across the shore and their cross-shore dynamics have been widely documented based on fieldwork, video imagery and tunnel experiments. These previous studies reveal the

relative stability of bars in low-energy environments (Boczar-Kanakiwicz and Davidson-Arnott, 1987; O'Hare and Huntley, 1994). On the contrary, the nearshore bars located in more energetic areas are mobile on both daily-to-annual and inter-annual time scales. Over short time scales, a significant correlation is generally found between offshore migration and the occurrence of larger waves (Sallenger et al., 1985; Soupy Alexander and Holman, 2004). At these scales, both onshore and offshore migrations are in evidence, with on- and offshore migration rates being related to wave energy (Wright et al., 1986; Masselink, 2004). Over the years, net seaward-cyclic migrating sandbars are observed at many sites (Shand et al., 2001; Van Enckevort and Ruessink, 2003a) with migration rates ranging from 0.1 to 0.5 m day⁻¹ on average. Due to the low space and time resolution of Spot records, it was difficult to get information on the net offshore migration and, more generally, on the across-shore variability of the nearshore bars that border the SW coast of France. On the contrary, alongshore non-uniform pattern variability was clearly shown by our data set. Furthermore, Spot imagery enabled us to consider a large number of rhythmic bars, which decreased the uncertainty of the measurements.

Fig. 6 summarizes the major outcome of this study. These preliminary results concerning sandbank morphology and dynamics require further interpretation. Four main issues are discussed herein.

The first question concerns the long-term persistence of the nearshore bars, which has been demonstrated using field surveys (De Melo Apoluceno et al., 2002). Intertidal-ridge decay, which is related to high-energy wave conditions (Davis et al., 1972; Wright and Short, 1984), has not been observed. Crescentic plan shapes are described as both temporarily and spatially mobile, and their decay is also related to energetic sea states (Bowman and Goldsmith, 1983; Van Enckevort and Ruessink, 2003b). In the future, their morphological behavior and short-to-mid term evolution along the SW

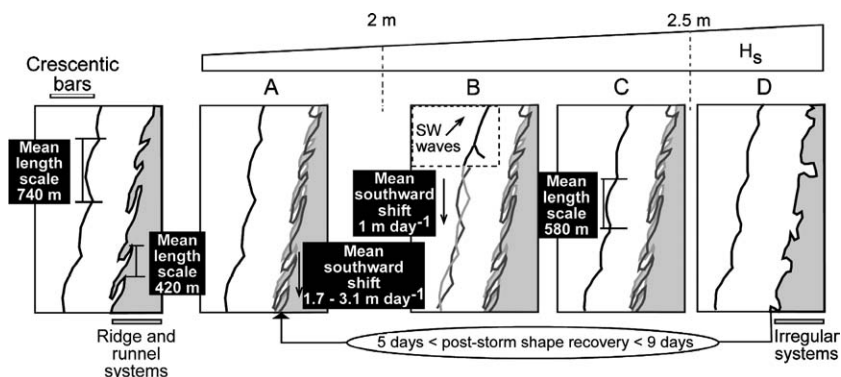


Fig. 6. Result summary. Rhythmic bar topography and migration rates are indicated as a function of significant wave height (H_s) to highlight thresholds determining abrupt or gradual changes. Time range for post-storm ridge and runnel shape recovery is also provided.

coast of France will be more accurately studied by obtaining continuous video images (Desmazes et al., 2002) and wave data records.

The second issue concerns the thresholds beyond which the bars undergo transformations. In the intertidal area, and up to H_s values of 2.5 m, the intertidal topography varied little, while the ridges and the runnels moved to the south (Fig. 6A), with a speed that increased with the H_s value and wave orientation, as was demonstrated by the impact of wave obliquity on the longshore current speed (see Section 3.2). When the mean H_s exceeded 2.5 m (Fig. 6D), the ridge morphology seemed to be damaged by the opening of troughs, which might be attributed to the rotation of existing runnels and/or the erosion rip-currents that were found to accompany rising sea states (Short, 1985). The crescents were affected by waves of at least 2 m H_s (Fig. 6B and C). Short-wave impact was more effective for wave heights that were smaller than 3 m, as demonstrated by the tests performed using SWAN and MORPHODYN nested models. Thus, the inner systems respond to calmer wave climate than the outer systems, which has also been demonstrated on Denmark coasts, in environments that are dominated by a smaller tidal range (0.3 m) and a less-energetic wave climate (mean annual wave height of 0.55 m with periods of 2.5–3.5 s) (Aagaard, 1991). In a mesotidal area characterized by a mean H_s of about 2.5 m, it has been demonstrated that offshore bars respond more significantly to changes in wave height, whereas inner bars seem to be shielded from incident-wave energy by breaking over the other bars (Soupy Alexander and Holman, 2004). This might explain why, considering analogous H_s values, the destruction of the ridges has not been observed along the SW coast of France.

The third issue concerns the time response of the bars. In low energetic areas, the bars are clearly visible during the first 2–3 days after the storm (Owens and Frobel, 1977). In the case of the SW coast of France, 4 days after the storm, the ridge and runnel systems were still not clearly organized. The ridge and runnel systems recovered their classical summer shape 5–9 days after the storm under mean wave-climate conditions.

Finally, as the fourth issue, the impact of high wave forcing on the crescentic bars is discussed. Waves with H_s higher than 2 m had at least three consequences. First, the bars moved, on average, in the longshore-drift direction if the resulting wave direction differed from that perpendicular to the bars. Simultaneous updrift- and downdrift-shifted bars have been observed. Ridge and runnel systems also showed the capacity to move with or against the flow, and both the rhythmic patterns were sometimes stationary. These combined behaviors have already been described at Duck, NC (Konicki and Holman, 2000) and at Noordwijk, The Netherlands (Van Enckevort and Ruessink, 2003b). Second, deep

morphological changes of the crescentic plan shapes associated with wave-incidence anomalies occasionally occurred. According to the data used for this study, an increased percentage of southwest waves seems to be able to alter the bar symmetry. However, in this particular case, asymmetric bars derived from the interaction between SW and NW waves, with the NW waves always remaining dominant features. Castelle and Bonneton (2004) demonstrated with a numerical approach that a long period of NW swells also induced the dissymmetric behavior of nearshore crescentic bars. Third, based on the yearly average wave climatology, it was found that the length scale of the crescentic bars was slightly negatively correlated with the mean wave height. If the crescentic bar alongshore length is linked to the development of rip cells (for example, Short, 1999) and as rip spacing increases with sea states (Short, 1985), the alongshore length of the crescentic bars is expected to increase with wave height. These different hypotheses will be evaluated soon by comparing directional and continuous wave-rider buoy records, which were recently started, to forthcoming crescent morphological maps. New records will also be helpful to analyze the time lag of the subtidal rhythmic systems to modifications of the wave climate that cannot be examined using this data set.

10. Conclusions

In this paper, a characterization of the alongshore morphodynamics of both the ridge and runnel systems and the crescentic bars that border the southwest coast of France was initiated by combining large-scale coastal mapping derived from high-resolution satellite measurements with a complete set of hydrodynamic data. About 35 km of coast was investigated, and, on average, 75 and 41 ridge and runnel systems and crescentic bars were studied, respectively. This work provides sound, although preliminary, arguments to explain the shape, alongshore dynamics and temporal variations of the length scale and the migration rates of these rhythmic coastal sedimentary patterns according to hydrodynamics and, particularly, wave climate. To summarize, the progressive influence of thresholds presenting increasing H_s values has been demonstrated.

Ridge and runnel systems were found in the intertidal area. When the mean offshore H_s was lower than 2.5 m, the ridge and runnel systems migrated southward by 1.7–3.1 m day⁻¹. When events of relatively high energy occurred (characterized by H_s values higher than 2.5 m and lasting for at least 24 h), randomly orientated runnels were observed and the rhythmic morphology was damaged. After a storm, the ridge and runnel topography was recovered within 5–9 days.

The crescentic bars were affected by waves with H_s values higher than 3 m (slightly less for short waves).

The occurrence of wave directional anomalies modified their original convex form into a more flattened shape. Depending on the wave orientation, the crescentic bars moved in the longshore-drift direction. Finally, it was shown that, on a yearly scale, the length scale of the crescentic bars decreased with increasing mean H_s .

Clearly, regardless of the wave-climate strength, the nearshore zone of the SW French coast is constantly modified, which requires the use of observation and interpretation tools with high acquisition frequencies. The complementary data provided will enable the precise determination of the energy and temporal scales to which the coastal dynamics are sensitive (for instance, the wave-action duration involving morphological changes in the intertidal domain). Also, they will allow more precise calculations of the sand-transport rate due to littoral drift, which was only approximated here because the wave direction is unfortunately lacking in the older databases. Finally, with the aim of simulating coastline morphodynamics, it will be necessary to better define the wave-height threshold beyond which the ridge morphology is modified. To conclude this paper, we must note that cross-shore morphodynamics, particularly of subtidal crescents, need to be studied in order to complete the analysis of the SW French coast morphodynamics. In addition, the interaction between the systems must be intensively investigated.

References

- Aagaard, T., 1991. Multiple-bar morphodynamics and its relation to low-frequency edge waves. *Journal of Coastal Research* 7, 801–813.
- Battjes, J.A., Janssen, J.P.F.M., 1978. Energy loss and setup due to breaking of random waves. In: *Proceedings of 19th International Conference of Coastal Engineering*, ASCE, pp. 569–587.
- Blondeaux, P., 2001. Mechanics of coastal forms. *Annual Review of Fluid Mechanics* 33, 339–370.
- Boczar-Kanakiewick, B., Davidson-Arnott, R.G.D., 1987. Nearshore bar formation by non-linear wave processes – a comparison of model results and field data. *Marine Geology* 77, 287–304.
- Bowman, D., Goldsmith, V., 1983. Bar morphology of dissipative beaches: an empirical model. *Marine Geology* 51, 15–33.
- Brander, R.W., Cowell, P.J., 2003. A trend-surface technique for discrimination of surf-zone morphology: Rip current channels. *Earth Surface Processes and Landforms* 28, 905–918.
- Butel, R., Dupuis, H., Bonneton, P., 2002. Spatial variability of wave conditions on the French Atlantic coast using in-situ data. *Journal of Coastal Research* SI 36, 96–108.
- Carter, D.J.T., 1982. Prediction of wave height and period for a constant wind velocity using the JONSWAP formulae. *Ocean Engineering* 9, 17–33.
- Castelle, B., Bonneton, P., 2004. Modélisation de la morphodynamique des plages d'Aquitaine. In: *Proceedings of the 8^{èmes} Journées Nationales Génie Côtier. Génie Civil*, Compiègne, France, September 2004.
- Coco, G., Burnet, T.K., Werner, B.T., Elgar, S., 2003. Test of self-organization in beach cusp formation. *Journal of Geophysical Research-Oceans* 108 (Art. No. 3101).
- Davies, J.L., 1972. *Geographical Variation in Coastal Development*. Oliver and Boyd, Edinburgh, 204 pp.
- Davis, R.A., Fox, W.T., Hayes, M.O., Boothroyd, J.C., 1972. Comparison of ridge and runnel systems in tidal and non-tidal environments. *Journal of Sedimentary Petrology* 2, 413–421.
- Davis Jr., R.A., Hayes, M.O., 1984. What is a wave dominated coast? *Marine Geology* 60, 313–329.
- De Melo Apoluceno, D., Howa, H., Dupuis, H., Oggian, G., 2002. Morphodynamics of ridge and runnel systems during summer. *Journal of Coastal Research* SI 36, 222–230.
- Desmazes, F., Michel, D., Howa, H., Pedreros, R., 2002. Etude morphodynamique du site atelier du Truc-Vert. In: *Proceedings of the 7^{èmes} Journées Nationales Génie Civil – Génie Côtier*, pp. 148–156.
- Froidefond, J.M., Gallissaires, J.M., Prud'homme, P., 1990. Spatial variation in sinusoidal wave energy on a crescentic nearshore bar; application to the Cap Ferret coast, France. *Journal of Coastal Research* 6, 927–942.
- Guillaume, A., 1987. VAG, modèle de prévision de l'état de la mer en eau profonde. Note de travail de l'E.E.R.M. N°. 178. Direction de la Météorologie Nationale, France, 128 pp.
- Konicki, K.M., Holman, R.A., 2000. The statistics and kinematics of transverse sand bars on an open coast. *Marine Geology* 169, 69–101.
- Lafon, V., De Melo Apoluceno, D., Dupuis, H., Michel, D., Howa, H., Froidefond, J.M., 2004. Morphodynamics of nearshore rhythmic sandbars in a mixed-energy environment (SW France): I. Mapping changes using visible satellite imagery. *Estuarine, Coastal and Shelf Science* 61, 289–299.
- Lafon, V., Dupuis, H., Howa, H., Froidefond, J.M., 2002a. Determining ridge and runnel longshore migration rate using SPOT imagery. *Oceanologica Acta* 25, 149–158.
- Lafon, V., Froidefond, J.M., Lahet, F., Castaing, P., 2002b. SPOT shallow water bathymetry of a moderately turbid tidal inlet based on field measurements. *Remote Sensing of Environment* 81, 136–148.
- Lorin, J., Viguier, J., Migniot, C., 1979. Etude en Nature de la Côte Aquitaine entre la Pointe de Grave et l'Embouchure de l'Adour. Unpublished report, L.C.H.F, Maison Alfort, France.
- Madsen, O.S., Poon, Y.-K., Graber, H.C., 1988. Spectral wave attenuation by bottom friction: theory. In: *Proceedings of the 21st International Conference of Coastal Engineering*. ASCE, pp. 492–504.
- Masselink, G., 2004. Formation and evolution of multiple intertidal bars on macrotidal beaches: application of a morphodynamic model. *Coastal Engineering* 51, 713–730.
- Michel, D., Howa, H., 1999. Short-term morphodynamic response of a ridge and runnel system on a mesotidal sandy beach. *Journal of Coastal Research* 15, 428–437.
- O'Hare, T.J., Huntley, D.A., 1994. Bar formation due to wave groups and associated long waves. *Marine Geology* 116, 313–325.
- Owens, E.H., Frobel, D.H., 1977. Ridge and runnel systems in the Magdalen Islands, Quebec. *Journal of Sedimentary Petrology* 47, 191–198.
- Pedreros, R., Howa, H., Michel, D., 1996. Application of grain-size-trend analysis for the determination of sediment transport pathways in intertidal areas. *Marine Geology* 135, 35–49.
- Saint-Cast, F., 2002. Modélisation de la morphodynamique des corps sableux en milieu littoral. PhD thesis, University of Bordeaux 1, Talence, France.
- Sallenger Jr., A.H., Holman, R.A., Birkemeier, W.A., 1985. Storm-induced response of a nearshore-bar system. *Marine Geology* 64, 237–257.
- Sénéchal, N., Dupuis, H., Bonneton, P., Howa, H., Pedreros, R., 2001. Irregular wave transformation in the surf zone over a gently sloping sandy beach. *Oceanologica Acta* 24 (6), 545–556.

- Shand, R.D., Bailey, D.G., Shepherd, M.J., 1999. An inter-site comparison of net offshore bar migration characteristics and environmental conditions. *Journal of Coastal Research* 15, 750–765.
- Shand, R.D., Bailey, D.G., Shepherd, M.J., 2001. Longshore realignment of shore-parallel sand-bars at Wanganui, New Zealand. *Marine Geology* 179, 147–161.
- Short, A.D., 1985. Rip-current type, spacing and persistence, Narrabeen Beach, Australia. *Marine Geology* 65, 47–71.
- Short, A.D., 1999. *Handbook of Beach and Shoreface Morphodynamics*. John Wiley & Sons LTD, UK, 379 pp.
- Short, A.D., Aagaard, T., 1993. Single and multi-bar beach change models. *Journal of Coastal Research* SI 15, 141–157.
- Soupy Alexander, O., Holman, R.A., 2004. Quantification of nearshore morphology based on video imaging. *Marine Geology* 208, 101–111.
- Van Enckevort, I.M.J., Ruessink, B.G., 2003a. Video observations of nearshore bar behaviour. Part 1: alongshore uniform variability. *Continental Shelf Research* 23, 501–512.
- Van Enckevort, I.M.J., Ruessink, B.G., 2003b. Video observations of nearshore bar behaviour. Part 2: alongshore non-uniform variability. *Continental Shelf Research* 23, 513–532.
- Wright, L.D., Nielsen, P., Shi, N.C., List, J.H., 1986. Morphodynamics of a bar-trough surf zone. *Marine Geology* 70, 251–285.
- Wright, L.D., Short, A.D., 1984. Morphodynamic variability of surf zones and beaches: a synthesis. *Marine Geology* 56, 93–118.